Cellular/Molecular

Involvement of Ca^{2+} Channel Synprint Site in Synaptic Vesicle Endocytosis

Hiroyasu Watanabe,[1] Takayuki Yamashita,[1] Naoto Saitoh,[2] Shigeki Kiyonaka,[3] Akihiro Iwamatsu,[4] Kevin P. Campbell,[5] Yasuo Mori,[3] and Tomoyuki Takahashi[1,2]

[1]Cellular and Molecular Synaptic Function Unit, Initial Research Project, Okinawa Institute of Science and Technology Promotion Corporation, Okinawa 904-2234, Japan, [2]Department of Neurophysiology, Doshisha University Faculty of Life and Medical Sciences, Kyoto 610-0394, Japan, [3]Laboratory of Molecular Biology, Department of Synthetic Chemistry and Biological Chemistry, Graduate School of Engineering, Kyoto University, Kyoto 615-8510, Japan, [4]Protein Research Network Inc., Kanagawa 236-0004, Japan, and [5]Howard Hughes Medical Institute, Departments of Molecular Physiology and Biophysics, Internal Medicine, and Neurology, University of Iowa Carver College of Medicine, Iowa City, Iowa 52242

The synaptic protein interaction (synprint) site of the voltage-gated Ca^{2+} channel (VGCC) α1 subunit can interact with proteins involved in exocytosis, and it is therefore thought to be essential for exocytosis of synaptic vesicles. Here we report that the synprint site can also directly bind the μ subunit of AP-2, an adaptor protein for clathrin-mediated endocytosis, in competition with the synaptotagmin 1 (Syt 1) C2B domain. In brain lysates, the AP-2–synprint interaction occurred over a wide range of Ca^{2+} concentrations but was inhibited at high Ca^{2+} concentrations, in which Syt 1 interacted with synprint site. At the calyx of Held synapse in rat brainstem slices, direct presynaptic loading of the synprint fragment peptide blocked endocytic, but not exocytic, membrane capacitance changes. We propose that the VGCC synprint site is involved in synaptic vesicle endocytosis, rather than exocytosis, in the nerve terminal, via Ca^{2+}-dependent interactions with AP-2 and Syt.

Introduction

In the nerve terminal, P/Q and N subtypes of voltage-gated Ca^{2+} channels (VGCCs) play pivotal roles in neurotransmitter release by providing pathways for Ca^{2+} entry (Luebke et al., 1993; Takahashi and Momiyama, 1993). VGCCs are also thought to play an additional role in synaptic vesicle exocytosis through direct interactions with syntaxin (Stx), SNAP-25, and synaptotagmin (Syt) at the so-called synprint site in a large intracellular loop between transmembrane domains II and III ($L_{II–III}$) of the VGCC α1 subunit (Sheng et al., 1996; Catterall, 2000). This synprint hypothesis has been supported by the finding that loading a synprint fragment peptide into presynaptic neurons inhibits synaptic transmission (Mochida et al., 1996; Rettig et al., 1997). However, the synprint fragment can also block the interaction between Syt 1 and AP-2 (Chapman et al., 1998), and Syt can participate in vesicle endocytosis (Poskanzer et al., 2003; Llinás et al., 2004) as well as exocytosis (Geppert et al., 1994). Furthermore, synaptic transmission can eventually be blocked by vesicle depletion after sustained block of endocytosis (Koenig and Ikeda, 1989; Yamashita et al., 2005). Thus, it remains possible that VGCC synprint might also be involved in vesicle endocytosis. Indeed, in cultured secretory cells, overexpression of a synprint site-deleted VGCC mutant protein inhibits both exocytic and endocytic membrane capacitance changes (Harkins et al., 2004). While screening for proteins that interact with the VGCC synprint site, we found that AP-2μ subunit can bind to it directly. This interaction competed with the Syt–synprint interaction (Chapman et al., 1998) in a Ca^{2+} concentration-dependent manner. When loaded into the calyx of Held presynaptic terminal in acute slices of rat brainstem, the synprint fragment peptide nearly abolished endocytic changes of membrane capacitance but surprisingly had no effect on exocytic capacitance changes. These results taken together point toward an endocytic, rather than an exocytic, role for the VGCC synprint site in vesicle recycling.

Materials and Methods

All experiments were performed in accordance with the guidelines of the Physiological Society of Japan.

Materials. cDNAs encoding rabbit N-type (GenBank accession number D14157), P/Q-type (GenBank accession number X57477), and L-type (GenBank accession number X15539) VGCCs were used for cloning deletion fragments. cDNAs encoding rat AP-2μ1 subunit (GenBank accession number M23674), Syt 1 (GenBank accession number X52772), and Stx 1a (GenBank accession number NM_053788) were obtained using reverse transcription-PCR from 7-d-old rat whole brains. The following vectors were used: pGEX4T-1 (GE Healthcare), pMAL–C2E (New England Biolabs), pCMV–Tag3 (Stratagene), and pEGFP–C (Clontech). The following antibodies were used: anti-$Ca_V2.2$ antibody (Alomone Labs); anti-β4 antibody (Kiyonaka et al., 2007); monoclonal antibody $VD2_1$, which recognizes all Ca^{2+} channel β subunits (Sakamoto and Campbell, 1991); anti-MBP antibody and anti-α-adaptin (clone 100/2) antibody (Sigma); anti-c-Myc antibody (9E10); anti-AP-2 antibody (AP-6; Calbiochem); anti-gamma adaptin (AP-1), anti-β-adaptin,

Received July 7, 2009; revised Oct. 27, 2009; accepted Nov. 11, 2009.

This study was supported by a Grant-in-Aid for Specially Promoted Research from the Ministry of Education, Culture, Sports, Science, and Technology. We thank Masayoshi Mishina, Takao Shimizu, and Kentaro Shiraki for technical advice, Idy Ko and Masakuni Yagi for technical assistance, and Ervin Johnson, Shigeo Takamori, and Kohji Takei for comments.

Correspondence should be addressed to Tomoyuki Takahashi, Department of Neurophysiology, Doshisha University Faculty of Life and Medical Sciences, Kyoto 610-0394, Japan. E-mail: ttakahas@oist.jp.

DOI:10.1523/JNEUROSCI.3214-09.2010

 0270-6474/10/300655-06$15.00/0

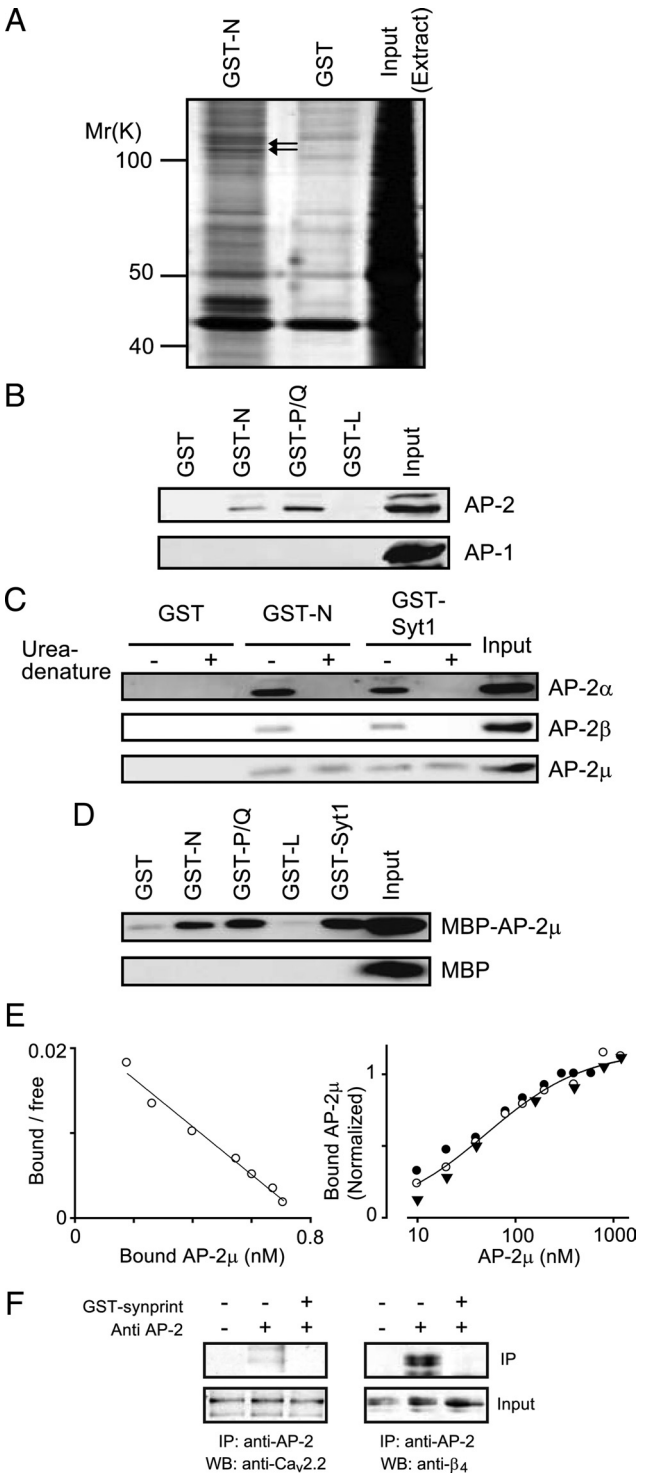

Figure 1. Direct interaction of AP-2μ with VGCC synprint site. ***A***, Affinity column chromatography for screening N-synprint-binding proteins. Brain extract from 7-d-old rats (Input) was loaded onto a GST- or GST–N-synprint-immobilized column. Bound proteins were eluted and analyzed by SDS-PAGE and silver staining. Two bands indicated by arrows were identified as AP-2αA (110 kDa) and AP-2αC (100 kDa), respectively, by mass spectrometry. ***B***, Eluates from the column with GST–N-synprint (718-963 aa, GST-N), GST–P/Q-synprint (715-1015 aa, GST-P/Q), and corresponding loop of GST–L–$L_{II–III}$ (800-910 aa, GST-L) were analyzed by immunoblot for AP-1 and AP-2. Standard was 15.6% of the input. ***C***, Pull-down assays using GST, GST–N-synprint, or GST–Syt1-C2B (248–421 aa, GST-Syt1), before (−) and after (+) urea denature of brain lysate. AP-2α, AP-2β, and AP-2μ were detected using their specific antibodies. Standard was 30% of the input. ***D***, *In vitro* binding assays using recombinant proteins (GST, GST-N, GST-P/Q, GST-L, GST-Syt1)-immobilized beads and MBP-fused AP-2μ subunit (123-435 aa). AP-2μ bindings were detected using anti-MBP antibody. Standard was 3% of the input. ***E***, Scatchard plot indicating concentration-dependent bindings of MBP–AP-2μ with GST–N-synprint. K_d was calculated from a linear regression line. Similar results were obtained from two other trials. In the right, data from three experiments were normalized and were fit by Hill plot (Hill coefficient of 0.85). ***F***, Coimmunoprecipitation (IP) of AP-2 with $Ca_V2.2$ (middle lane in the left) or β4 (middle lane in the right) subunit of native VGCC in heparin-purified samples of brain tissue. VGCC subunits in starting samples are shown in Western blot (WB) in the bottom row. Standard was 2% of the input. GST–N-synprint disrupted the interactions of AP-2 with $Ca_V2.2$ and β4 subunits, respectively (right lanes).

and anti-AP-50 (AP-2μ) antibodies (BD Transduction Laboratories); anti-Syt antibody (SYA148; Nventa Biopharmaceuticals); anti-Stx1 antibody (MBL International); and anti-enhanced green fluorescent protein (EGFP) antibody (Invitrogen). Recombinant fusion proteins were purified according to the protocol of the manufacturer. Glutathione *S*-transferase (GST)-fusion and MBP-fusion proteins were dialyzed against 20 mM Tris, 1 mM EDTA, and 1 mM DTT, pH 7.5, at 4°C. To prepare rat brain lysate, whole brains of 7-d-old rats were homogenized in 20 mM Tris, 1 mM EGTA, 150 mM NaCl, 1% NP-40, and a protease inhibitor cocktail (Roche). Homogenates were then sonicated and centrifuged at 3000 × *g* for 10 min. Supernatants were collected and further centrifuged at 10,000 × *g* for 20 min to be used for the following experiments.

Biochemistry. In affinity column chromatography, GST-fusion proteins were immobilized on glutathione Sepharose 4B (GSH) beads (GE Healthcare) and packed into a column. Brain lysates prepared from 7-d-old Wistar rats were passed through a filter (0.45 μm), and the filtrated lysates were passed through a GST column before they were applied to sample columns. After washing the sample columns with a buffer solution (20 mM Tris, 1 mM EDTA, 150 mM NaCl, and 1% NP-40), binding proteins were eluted by a 500 mM NaCl containing buffer solution. Eluted samples were treated with SDS sample buffer (60 mM Tris, 2% SDS, 10% glycerol, and 250 mM 2-mercaptoethanol) and submitted to silver staining or immunoblot analysis. *In vitro* binding assays were performed using GST-fusion proteins immobilized onto GSH-beads in separate tubes. The immobilized beads were incubated with MBP-fusion proteins in buffer with 1 mM DTT and 0.2 mg/ml BSA at 4°C for 2 h. After washing the beads four times with the buffer, they were suspended in SDS buffer. The bead-bound proteins were subjected to immunoblot analysis with anti-MBP antibody. Ca^{2+} buffers of different concentrations were prepared using 1 mM EGTA according to the online protocol (http://www.stanford.edu/~cpatton/maxc.html). For urea denature of brain lysate (Fig. 1*C*), brain lysates (6 mg/ml) were incubated with 7.5 M urea for 15 min at room temperature and then diluted fivefold into PBS containing 1% Triton X-100. Beads were washed five times with 4 vol of buffer. For immunoprecipitation assay (Fig. 1*F*), anti-AP-2 antibody (4 μg) was immobilized on protein A agarose beads and then incubated with 800 μl aliquots of the heparin-purified samples (1 mg of proteins) for 4 h at 4°C. Native VGCC complexes were partially purified from C57BL/6 mouse whole brain and submitted to immunoprecipitation assays as reported previously (Kiyonaka et al., 2007). To disrupt the native AP-2–VGCC association, partially purified VGCC complexes were incubated with 450 nM GST–N-synprint (718-963 aa) at 4°C for 8 h. Mass spectrometry analysis was performed as reported previously (Nishimura et al., 2006).

Electrophysiology. Whole-cell recordings and membrane capacitance (C_m) measurements were performed at room temperature (22–25°C) at the calyx of Held presynaptic terminals in auditory brainstem slices (200 μm thick) containing the medial nucleus of trapezoid body prepared from 7- to 8-d-old Wistar rats as described previously (Yamashita et al., 2005). The extracellular solution contained 115 mM NaCl, 10 mM tetraethylammonium Cl, 2.5 mM KCl, 1 mM $MgCl_2$, 2 mM $CaCl_2$, 26 mM $NaHCO_3$, 1.25 mM NaH_2PO_4, 10 mM glucose, 0.5 mM ascorbic acid, 3 mM *myo*-inositol, 2 mM sodium pyruvate, 1 μM tetrodotoxin, 0.5 mM 4-aminopyridine, 10 μM bicuculline methiodide, and 0.5 μM strychnine hydrochloride (pH 7.4 when bubbled with 95% O_2 and 5% CO_2). Patch pipettes (6–8 MΩ) had a series resistance of 11–27 MΩ, which was compensated by up to 75% for its final value to be 6.7–7.0 MΩ. Pipette solution contained the following (in mM): 109 CsCl, 40 HEPES, 0.5

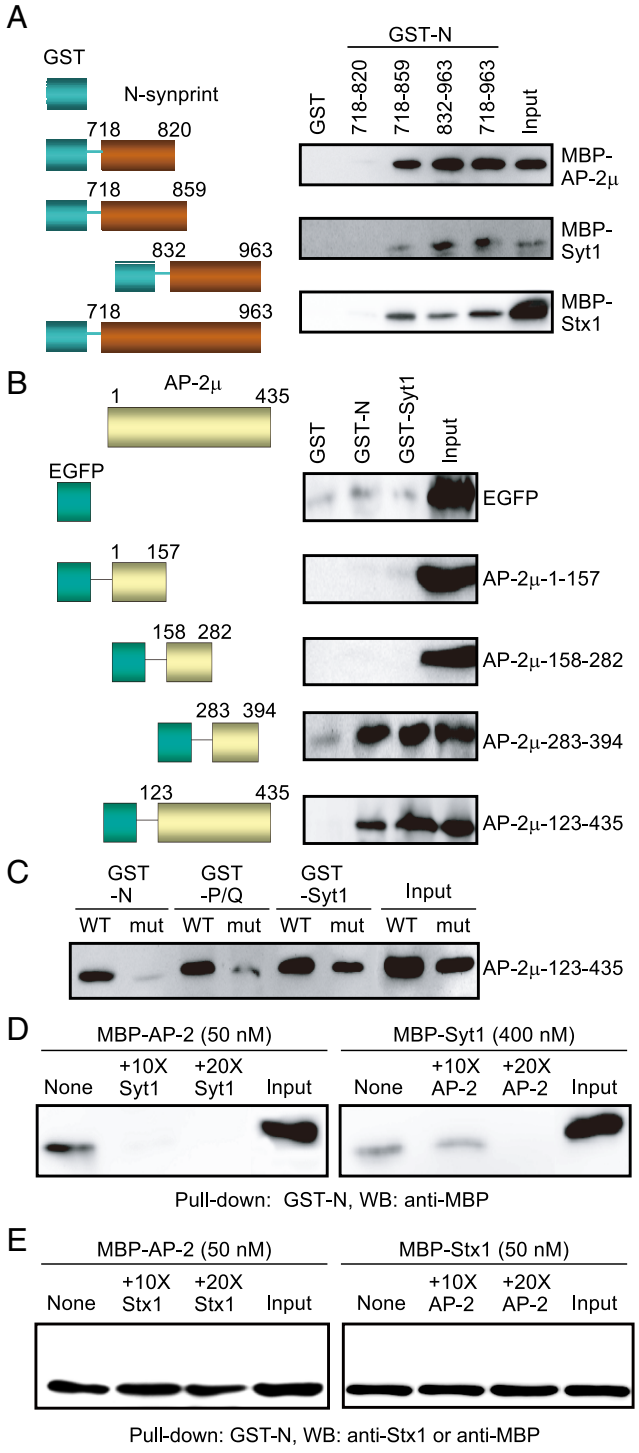

Figure 2. The common binding region of VGCC synprint site, shared by AP-2μ and Syt 1 C2B domain. ***A***, Narrowing down the binding region of N-synprint for AP-2μ, Syt 1, and Stx 1 by pull-down assay using GST–N-synprint fragments (left). Their bindings to MBP-fused AP-2μ (standard was 2.2% of the input), Syt 1 C2B (248-421 aa; standard was 2% of the input), or Stx 1 (1-288 aa; standard was 5% of the input) were analyzed using anti-MBP antibody. ***B***, Narrowing down the binding region of AP-2μ for binding to N-synprint and Syt1 C2B. GST or GST-fusion proteins were incubated with cell lysates obtained from COS 7 cells transfected with EGFP-fused AP-2μ fragments (left). Binding was evaluated by immunoblotting using anti-EGFP antibody (right). Standard was 33% of the input. ***C***, Reduced binding of two-points mutants (Y344A, K354A) of AP-2μ to N-synprint (GST-N), P/Q-synprint (GST-P/Q), and Syt 1 C2B (GST-Syt 1). Myc tag-fused wild-type (WT) and mutant (mut) AP-2μ subunits overexpressed in COS7 cells were pulled down, and their binding was detected using anti-Myc tag antibody. Standard was 30% of the input. ***D***, Competitions between AP-2μ and Syt for binding to N-synprint. Left, MBP–AP-2μ (50 nM) was pulled down by GST–N-synprint alone (None) or in the presence of MBP–Syt (1-421 aa) at 500 nM (10×) or at 1 μM (20×). Standard was 5% of the input. Right, MBP–Syt 1 (400 nM) was pulled down by GST–N-synprint alone (None) or in the presence of MBP–AP-2μ at 4 μM (10×) or at 8 μM (20×). Standard was 1% of the input. ***E***, Competitions between AP-2μ and Stx for binding to N-synprint. Left, MBP–AP-2μ alone (50 nM; None) or in the presence of MBP–Stx 1 at 500 nM (10×) or at 1 μM (20×). Standard was 10% of the input. Right, MBP–Stx 1 alone (50 nM; None) or in the presence of MBP–AP-2μ at 500 nM (10×) or at 1 μM (20×), Standard was 10% of the input. Experiments were performed in nominally Ca^{2+}-free media.

EGTA, 1 $MgCl_2$, 12 Na_2-phosphocreatine, 3 Mg-ATP, and 0.3 Na-GTP (pH 7.3–7.4 adjusted with CsOH). GST–N-synprint peptide or GST–$L_{II–III}$ peptide was included in the pipette solution, together with trehalose (0.2–1 mM) to minimize protein aggregations (Singer and Lindquist, 1998). These proteins (5 μM) were infused into presynaptic terminals, by gently applying blows of positive pressure, while the series resistance was maintained below 12 MΩ, 10 min before the start of recordings. The C_m analysis was made as described previously (Yamashita et al., 2005). Briefly, C_m changes within 200 ms after depolarizing pulse were excluded from analysis to avoid contaminations of conductance-dependent capacitance artifacts. The ΔC_m amplitude was measured as a difference between the baseline and at 200–250 ms after depolarization. For $C_m > 40$ s, regression line, obtained from baseline 0.005–10 s before stimulation, was subtracted (Yamashita et al., 2005).

Results

Direct interaction of VGCC synprint with AP-2μ

To identify proteins that interact with VGCC synprint site, we applied juvenile rat brain tissue lysate to an affinity column with GST-fused N-type VGCC synprint fragment (N-synprint). Proteins with the relative molecular masses of 110 and 100 kDa specifically bound to N-synprint (Fig. 1*A*). Matrix-assisted laser desorption/ionization time-of-flight mass spectrometry analysis indicated that these proteins were the AP-2αA and AP-2αC components of the clathrin adaptor AP-2 complex. Affinity columns showed binding of AP-2 complex to N-synprint, as well as to the synprint fragment of P/Q-type VGCC (P/Q-synprint) but not to the II–III loop domain of L-type VGCC (L–$L_{II–III}$) (Fig. 1*B*). In contrast, AP-1, a related adaptor protein, showed no binding to these fragments. Pull-down assays using urea-denatured brain lysate (Haucke et al., 2000) showed that N-synprint bound to the AP-2μ subunit but not to the AP-2α or AP-2β subunits (Fig. 1*C*). MBP-fused recombinant AP-2μ showed direct binding to N- or P/Q-synprint, as well as to Syt 1 C2B domain (Fig. 1*D*). The binding of AP-2μ to N-synprint was concentration dependent, with its K_d being estimated, by scatchard analysis, to be 30.8 ± 5.6 nM ($n = 3$) (Fig. 1*E*). Thus, AP-2μ subunit directly binds to the VGCC synprint site *in vitro*. In purified mouse brain lysates (Kiyonaka et al., 2007), native AP-2 could coimmunoprecipitate with $Ca_V2.2$ or VGCC β-subunit complexes (Fig. 1*F*) but not with $Ca_V1.2$ complex (supplemental Fig. S1, available at www.jneurosci.org as supplemental material). These interactions could be blocked by addition of GST–N-synprint (Fig. 1*F*). These results suggest that native AP-2 and VGCCs in the brain interact with each other.

Competitive binding of AP-2 and Syt 1 to VGCC

We next searched for the binding regions of AP-2μ and N-synprint in pull-down assays. MBP-tagged AP-2μ showed binding to the N-synprint amino acid fragments 718–859, 832–963, and 718–963 but not to 718–820 (Fig. 2*A*). These regions are in common with those involved in the binding of N-synprint to Syt 1 and Stx 1 (Fig. 2*A*). Among AP-2μ deletion mutants,

AP-2μ 283–394 showed binding to N-synprint (Fig. 2*B*). This fragment also showed bindings to Syt 1 C2B, as reported previously (Haucke et al., 2000). However, mutating AP-2μ tyrosine-344 and lysine-354 to alanine (Y344A and K354A) impaired the binding of AP-2μ 123–435 to N- and P/Q-synprint (Fig. 2*C*), as well as to Syt 1 C2B (Haucke et al., 2000), albeit to a lesser extent (Fig. 2*C*). In binding assay, Syt 1 competed off the AP-2μ–N-synprint binding and vice versa (Fig. 2*D*). It has been reported that mutations of Syt1 C2B domain at lysine-326 and alanine-327 abolishes bindings between AP-2, Syt1 C2B, and the synprint site (Chapman et al., 1998). Thus, AP-2μ, Syt 1 C2B, and the synprint site share common binding regions for their mutual interactions. In contrast, no competition was observed between Stx 1 and AP-2μ for binding to the synprint site (Fig. 2*E*) (supplemental Fig. S2, available at www.jneurosci.org as supplemental material).

Ca^{2+} dependence of VGCC/AP-2/Syt 1 interaction

The interaction between the VGCC synprint site and Stx is Ca^{2+} dependent (Sheng et al., 1996). To test whether the interactions between N-synprint and AP-2 or Syt 1 were also Ca^{2+} dependent, we performed pull-down assays at different Ca^{2+} concentrations ($[Ca^{2+}]$). AP-2μ showed binding to N-synprint at a wide range of $[Ca^{2+}]$. However, the binding decreased as $[Ca^{2+}]$ was elevated and became undetectable at 2 mM $[Ca^{2+}]$ (Fig. 3*A*). In contrast, Syt 1 showed binding to N-synprint only at >100 μM $[Ca^{2+}]$ (Fig. 3*A*). When Ca^{2+} was replaced by Sr^{2+} or Ba^{2+}, N-synprint still showed binding to AP-2 but no longer to Syt 1 (Fig. 3*B*), and no concentration dependence was observed for Sr^{2+} or Ba^{2+} for the AP-2–synprint interaction. In the absence of brain lysate, however, binding of recombinant AP-2μ to N-synprint showed no Ca^{2+} dependence (Fig. 3*C*). Given that the synprint–Syt 1 interaction is strengthened by Ca^{2+}-dependent oligomerization of Syt 1 at 50 μM to 1 mM $[Ca^{2+}]$ (Chapman et al., 1998; Wu et al., 2003; Grass et al., 2004), the apparent Ca^{2+} dependence of the AP-2μ–synprint interaction in brain lysate likely arose from competition between AP-2μ and Syt 1 for binding to the synprint site (Fig. 3*C*). However, it cannot be ruled out that an additional factor contained in brain lysate might confer the Ca^{2+} dependence.

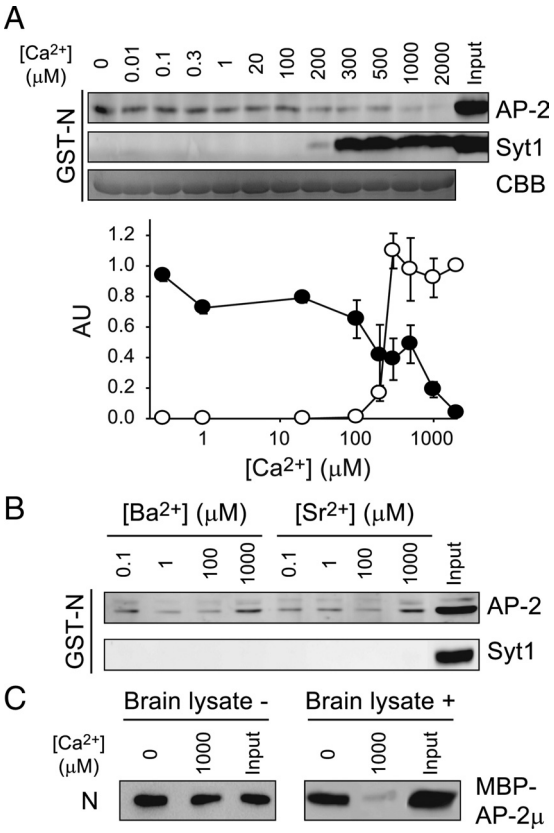

Figure 3. Ca^{2+} concentration-dependent binding of VGCC synprint site to AP-2μ and Syt. ***A***, Rat brain extracts were dissolved in Ca^{2+} buffers of various free Ca^{2+} concentrations and mixed with GST–N-synprint-bound beads. Top, Binding of AP-2μ and Syt were detected using anti-AP-2α (top row) or anti-Syt 1 (middle row) antibody, respectively. Standard was 14% of the input. Bottom row shows CBB stainings of bead-bound GST–N-synprint proteins. Bottom, Densitometric quantifications of binding intensities (ordinate in an arbitrary scale) at different Ca^{2+} concentrations (abscissa) for AP-2μ (filled circles) and Syt 1 (open circles). Vertical bars indicate SEMs of three experiments. ***B***, Effects of Ba^{2+} and Sr^{2+} on bindings of N-synprint to AP-2μ (top row) and Syt 1 (bottom row). Standard was 14% of the input. ***C***, Recombinant AP-2μ was incubated with N-synprint in 1 mM (1000) or 0 mM Ca^{2+} (0) in the presence (right) or absence (left) of brain extract. Binding of AP-2μ to N-synprint was detected using anti-MBP antibody. Standard was 20% of the input.

Involvement of VGCC synprint in endocytosis

An N-type VGCC synprint site fragment (N-synprint) blocks synaptic transmission when injected into cultured presynaptic neurons (Mochida et al., 1996; Rettig et al., 1997). This effect could, in principle, be caused by a block of exocytosis, endocytosis, or a combined impairment of these processes. This peptide fragment could also inhibit multiple intermolecular interactions, in which VGCC synprint and its interacting proteins are involved. To reexamine the effect of this peptide, we loaded N-synprint fragment (832–963 aa, 5 μM) into the calyx of Held presynaptic terminals and tested whether exocytosis and/or endocytosis of synaptic vesicles were affected, using C_m measurements (Sun and Wu, 2001; Yamashita et al., 2005). To minimize secondary effects caused by changes in vesicle recycling (Yamashita et al., 2005), we restricted our analysis of C_m changes (ΔC_m) to the first to fifth events induced by presynaptic Ca^{2+} currents (I_{pCa}) 10–20 min after peptide loading. In this condition, the N-synprint fragment slightly increased exocytic ΔC_m, concomitantly with an increase in I_{pCa} amplitude (Fig. 4*A*,*B*). In addition, N-synprint fragment loading markedly blocked endocytic C_m decay (Fig. 4*C*). Loading of GST–L–$L_{II–III}$ fragment had no such effects. The facilitatory effect of synprint fragment on I_{pCa} (Fig. 4*A*,*B*) is consistent with the idea that interaction of Stx with the synprint site regulates I_{pCa} (Stanley and Mirotznik, 1997). Consistent with this interpretation, readjustment of the I_{pCa} amplitude in N-synprint fragment-loaded terminals back to the control level abolished the exocytic ΔC_m increase. Thus, the target of the N-synprint fragment at this nerve terminal was I_{pCa} and vesicle endocytosis but not vesicle exocytosis.

Discussion

In the nerve terminal, synaptic vesicles are docked on an active zone of 200–300 nm in diameter, in which VGCCs are thought to be inserted within a distance of 20–200 nm from synaptic vesicles (Neher, 1998; Meinrenken et al., 2002). Ca^{2+} entry through 1–60 VGCCs (Stanley, 1993; Borst and Sakmann, 1996) can trigger single vesicle fusion for exocytic release of neurotransmitter. After fusion, a variety of endocytic proteins are assembled for clathrin-mediated vesicle endocytosis, in which the adaptor protein AP-2 plays an essential role (Schmid, 1997). Our present results suggest that VGCC synprint sites anchor a fraction of AP-2 complex, which is likely linked to the plasma membrane via interactions with phosphatidylinositol 4,5-bisphosphate

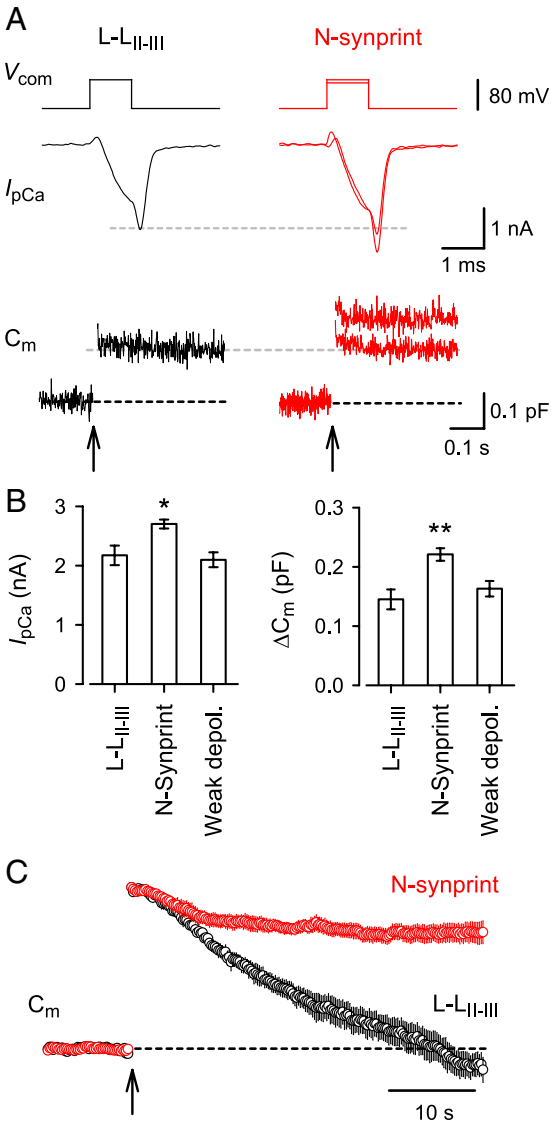

Figure 4. Effects of intraterminal loadings of N-synprint fragment on vesicle exocytosis and endocytosis at the calyx of Held. ***A***, Sample records of I_{pCa} and C_m changes induced by a 1 ms depolarizing command voltage pulse (V_{com}; from −80 to 0 mV), in the presence of GST–N-synprint (5 μM; red) or GST–L–L$_{II–III}$ (5 μM, black) in the presynaptic pipette. Middle column, In the presence of GST–N-synprint fragment, command pulse amplitude was reduced (by 5–10 mV) to match the I_{pCa} amplitude to that in GST–L–L$_{II–III}$ (superimposed). Arrows indicate the onset of command pulse in ***A*** and ***C***. Gray lines indicate the level of I_{pCa} amplitude and ΔC_m in control. ***B***, The mean amplitude of I_{pCa} (left) and ΔC_m (right) in the terminals loaded with GST–L–L$_{II–III}$ ($n = 10$; black) or GST–N-synprint ($n = 18$; red). Terminals loaded with GST–N-synprint showed significantly larger I_{pCa} (*$p < 0.02$) and ΔC_m (**$p < 0.002$) than GST–L–L$_{II–III}$-loaded terminals. When I_{pCa} in the terminal loaded with GST–N-synprint was matched to that with GST–L–L$_{II–III}$ (Weak depol.), ΔC_m was similar to that in the terminal loaded with GST–L–L$_{II–III}$ ($n = 7$, $p > 0.4$). ***C***, Presynaptic C_m change, induced by the 1 ms depolarizing pulse, shown in slow timescale. Averaged C_m traces, in the presence of GST–N-synprint (red; $n = 6$) or GST–L–L$_{II–III}$ (black; $n = 6$) in the recording patch pipette, were superimposed, after normalizing at 200–250 ms from the pulse onset.

(McPherson et al., 2008). This synprint-AP-2 interaction occurs for both N- and P/Q-type VGCCs but is not entirely universal because VGCCs in invertebrates such as *Drosophila* and *Caenorhabditis elegans* lack synprint sites (Littleton and Ganetzky, 2000; Spafford et al., 2003). At *Drosophila* neuromuscular junctions, the AP-2 complex forms a network surrounding the active zone (González-Gaitán and Jäckle, 1997), in which clathrin-mediated vesicle endocytosis occurs (Roos and Kelly, 1999). At the amphibian neuromuscular junction, clathrin-mediated vesicle endocytosis occurs in the area close to active zone, supporting the existence of local exo-endocytic cycling pool of vesicles (Teng and Wilkinson, 2000). It remains to be seen where exactly VGCCs are localized in the active zone. With respect to the coupling role of VGCCs for exocytosis and endocytosis of synaptic vesicles, it might be most efficient if they are localized at the periphery of the active zone.

Clathrin coating of vesicles is initiated by the interaction of AP-2 with Syt (Schmid, 1997). Their interactions are supposedly promoted by stonin, which binds to both AP-2 and Syt (Diril et al., 2006). Given that the VGCC synprint site can bind to Syt only at high Ca^{2+} concentrations (Fig. 3), it may be speculated that VGCCs sequentially interact with AP-2 and Syt during transient increases in Ca^{2+} concentration in and around the active zone. These interactions may promote the dynamic assembly of AP-2 and Syt. In this regard, Ca^{2+}-dependent binding of the VGCC C terminal to endophilin, an endocytic protein that interacts with dynamin, has been suggested previously to promote vesicle endocytosis (Chen et al., 2003).

The importance of Ca^{2+} in slow vesicle endocytosis is variable between preparations. At immature calyces of Held, it has been reported recently that slow vesicle endocytosis, lasting tens of seconds, requires a high concentration of Ca^{2+}, which can only be attained within a Ca^{2+} microdomain (Hosoi et al., 2009). Given that the Ca^{2+} concentration in the microdomain returns to the baseline within 10 ms (Neher, 1998), Ca^{2+} must play only a triggering role for the subsequent slow steps toward vesicle endocytosis. In our present study, intraterminal loading of the synprint fragment blocked endocytic capacitance changes but spared an initial recovery phase lasting several seconds (Fig. 4). A similar blocking effect, which spares the initial phase of endocytosis, has been observed for dynamin 1 proline-rich domain peptide (Yamashita et al., 2005). Thus, the initial endocytic component might be independent of clathrin and/or dynamin. In HeLaM cells, clathrin-mediated endocytosis can still be observed after ablating AP-2 proteins down to undetectable levels (Motley et al., 2003). Thus, also at the calyx of Held, AP-2-independent clathrin-mediated endocytosis might underlie the initial phase of endocytosis.

At resting Ca^{2+} concentrations, VGCC synprint sites can directly bind to AP-2μ (Figs. 1, 3), whereas at higher Ca^{2+} concentrations, they can bind to Stx (Sheng et al., 1996) and Syt 1 (Fig. 3) (Grass et al., 2004). Syt 1 and AP-2 also bind to each other (Zhang et al., 1994; Haucke et al., 2000; Grass et al., 2004). Thus, the synprint fragment peptide loaded into nerve terminals must interfere with the triplet interactions between the VGCC synprint site, AP-2μ, and Syt 1 C2B. Syt 1 C2B is thought to regulate the endocytic rate (Poskanzer et al., 2006). Genetic ablation of Syt 1 or its C2B domain slows the endocytic rate at cultured hippocampal synapses (Nicholson-Tomishima and Ryan, 2004) and at *Drosophila* neuromuscular junction (Poskanzer et al., 2006), supporting the endocytic role of Syt1 (Poskanzer et al., 2003; Llinás et al., 2004). Thus, the blocking effect of synprint fragment peptide loading on endocytosis observed at the calyx of Held (Fig. 4) can, at least in part, be explained by its inhibitory effect on the Syt–AP-2 interaction (Haucke et al., 2000). However, compared with mild blocking effects on endocytosis reported for Syt 1-null mutations (Nicholson-Tomishima and Ryan, 2004; Poskanzer et al., 2006), much stronger blocking effects on endocytosis are observed for synprint fragment loaded into the calyx terminal (Fig. 4). This suggests that interactions between the VGCC synprint

site, AP-2, and Syt may additionally be involved in vesicle endocytosis (Fig. 3).

Despite the fact that N-synprint can bind to the exocytic proteins Stx and Syt (Fig. 2) (Sheng et al., 1996, 1997), the N-synprint fragment peptide had no direct inhibitory effect on exocytosis at the calyx of Held in acute brainstem slices of immature rats (Fig. 4). Because the peptide blocked endocytosis, it is suggested that previously reported block of transmitter release by N-synprint peptide at cultured synapses (Mochida et al., 1996; Rettig et al., 1997) might be a secondary effect caused by the arrest of vesicle endocytosis and recycling (Koenig and Ikeda, 1989; Yamashita et al., 2005). However, our results cannot preclude the possibility that the VGCC synprint site might become involved in vesicle exocytosis at mature synapses.

References

Borst JG, Sakmann B (1996) Calcium influx and transmitter release in a fast CNS synapse. Nature 383:431–434.

Catterall WA (2000) Structure and regulation of voltage-gated Ca^{2+} channels. Annu Rev Cell Dev Biol 16:521–555.

Chapman ER, Desai RC, Davis AF, Tornehl CK (1998) Delineation of the oligomerization, AP-2 binding, and synprint binding region of the C2B domain of synaptotagmin. J Biol Chem 273:32966–32972.

Chen Y, Deng L, Maeno-Hikichi Y, Lai M, Chang S, Chen G, Zhang JF (2003) Formation of an endophillin-Ca^{2+} channel complex is critical for clathrin-mediated synaptic vesicle endocytosis. Cell 115:37–48.

Diril MK, Wienisch M, Jung N, Klingauf J, Haucke V (2006) Stonin 2 is an AP-2-dependent endocytic sorting adaptor for synaptotagmin internalization and recycling. Dev Cell 10:233–244.

Geppert M, Goda Y, Hammer RE, Li C, Rosahl TW, Stevens CF, Südhof TC (1994) Synaptotagmin I: a major Ca^{2+} sensor for transmitter release at a central synapse. Cell 79:717–727.

González-Gaitán M, Jäckle H (1997) Role of *Drosophila* α-adaptin in presynaptic vesicle recycling. Cell 88:767–776.

Grass I, Thiel S, Höning S, Haucke V (2004) Recognition of a basic AP-2 binding motif within the C2B domain of synaptotagmin is dependent on multimerization. J Biol Chem 279:54872–54880.

Harkins AB, Cahill AL, Powers JF, Tischler AS, Fox AP (2004) Deletion of the synaptic protein interaction site of the N-type ($Ca_V2.2$) calcium channel inhibits secretion in mouse pheochromocytoma cells. Proc Natl Acad Sci U S A 101:15219–15224.

Haucke V, Wenk MR, Chapman ER, Farsad K, De Camilli P (2000) Dual interaction of synaptotagmin with μ2- and α-adaptin facilitates clathrin-coated pit nucleation. EMBO J 19:6011–6019.

Hosoi N, Holt M, Sakaba T (2009) Calcium dependence of exo- and endocytotic coupling at a glutamatergic synapse. Neuron 63:216–229.

Kiyonaka S, Wakamori M, Miki T, Uriu Y, Nonaka M, Bito H, Beedle AM, Mori E, Hara Y, De Waard M, Kanagawa M, Itakura M, Takahashi M, Campbell KP, Mori Y (2007) RIM1 confers sustained activity and neurotransmitter vesicle anchoring to presynaptic Ca^{2+} channels. Nat Neurosci 10:691–701.

Koenig JH, Ikeda K (1989) Disappearance and reformation of synaptic vesicle membrane upon transmitter release observed under reversible blockage of membrane retrieval. J Neurosci 9:3844–3860.

Littleton JT, Ganetzky B (2000) Ion channels and synaptic organization: analysis of the *Drosophila* genome. Neuron 26:35–43.

Llinás RR, Sugimori M, Moran KA, Moreira JE, Fukuda M (2004) Vesicular reuptake inhibition by a synaptotagmin I C2B domain antibody at the squid giant synapse. Proc Natl Acad Sci U S A 101:17855–17860.

Luebke JI, Dunlap K, Turner TJ (1993) Multiple calcium channel types control glutamatergic synaptic transmission in the hippocampus. Neuron 11:895–902.

McPherson PS, Ritter B, Augustine GJ (2008) The molecular machinery for synaptic vesicle endocytosis. In: Structure and functional organization of the synapse (Hell JW, Ehlers MD, eds). New York: Springer.

Meinrenken CJ, Borst JG, Sakmann B (2002) Calcium secretion coupling at calyx of Held governed by nonuniform channel-vesicle topography. J Neurosci 22:1648–1667.

Mochida S, Sheng ZH, Baker C, Kobayashi H, Catterall WA (1996) Inhibition of neurotransmission by peptides containing the synaptic protein interaction site of N-type Ca^{2+} channels. Neuron 17:781–788.

Motley A, Bright NA, Seaman MN, Robinson MS (2003) Clathrin-mediated endocytosisin AP-2-depelted cells. J Cell Biol 162:909–918.

Neher E (1998) Vesicle pools and Ca^{2+} microdomains: new tools for understanding their roles in neurotransmitter release. Neuron 20:389–399.

Nicholson-Tomishima K, Ryan TA (2004) Kinetic efficiency of endocytosis at mammalian CNS synapses requires synaptotagmin 1. Proc Natl Acad Sci U S A 101:16648–16652.

Nishimura T, Yamaguchi T, Tokunaga A, Hara A, Hamaguchi T, Kato K, Iwamatsu A, Okano H, Kaibuchi K (2006) Role of numb in dendritic spine development with a Cdc42 GEF intersectin and EphB2. Mol Biol Cell 17:1273–1285.

Poskanzer KE, Marek KW, Sweeney ST, Davis GW (2003) Synaptotagmin 1 is necessary for compensatory synaptic vesicle endocytosis *in vivo*. Nature 426:559–563.

Poskanzer KE, Fetter RD, Davis GW (2006) Discrete residues in the C_2B domain of synaptotagmin I independently specify endocytic rate and synaptic vesicle size. Neuron 50:49–62.

Rettig J, Heinemann C, Ashery U, Sheng ZH, Yokoyama CT, Catterall WA, Neher E (1997) Alteration of Ca^{2+} dependence of neurotransmitter release by disruption of Ca^{2+} channel/syntaxin interaction. J Neurosci 17:6647–6656.

Roos J, Kelly RB (1999) The endocytic machinery in nerve terminals surrounds sites of exocytosis. Curr Biol 9:1411–1414.

Sakamoto J, Campbell KP (1991) A monoclonal antibody to the β subunit of the skeletal muscle dihydropyridine receptor immunoprecipitates the brain ω-conotoxin GVIA receptor. J Biol Chem 266:18914–18919.

Schmid SL (1997) Clathrin-coated vesicle formation and protein sorting: an integrated process. Annu Rev Biochem 66:511–548.

Sheng ZH, Rettig J, Cook T, Catterall WA (1996) Calcium-dependent interaction of N-type calcium channels with the synaptic core complex. Nature 379:451–454.

Sheng ZH, Yokoyama CT, Catterall WA (1997) Interaction of the synprint site of N-type Ca^{2+} channels with the C2B domain of synaptotagmin I. Proc Natl Acad Sci U S A 94:5405–5410.

Singer MA, Lindquist S (1998) Thermotolerance in *Saccharomyces cerevisiae*: the yin and yang of trehalose. Trends Biotechnol 16:460–468.

Spafford JD, Munno DW, Van Nierop P, Feng ZP, Jarvis SE, Gallin WJ, Smit AB, Zamponi GW, Syed NI (2003) Calcium channel structural determinants of synaptic transmission between identified invertebrate neurons. J Biol Chem 278:4258–4267.

Stanley EF (1993) Single calcium channels and acetylcholine release at a presynaptic terminal. Neuron 11:1007–1011.

Stanley EF, Mirotznik RR (1997) Cleavage of syntaxin prevents G-protein regulation of presynaptic calcium channels. Nature 385:340–343.

Sun JY, Wu LG (2001) Fast kinetics of exocytosis revealed by simultaneous measurements of presynaptic capacitance and postsynaptic currents at a central synapse. Neuron 30:171–182.

Takahashi T, Momiyama A (1993) Different types of calcium channels mediate central synaptic transmission. Nature 366:156–158.

Teng H, Wilkinson RS (2000) Clathrin-mediated endocytosis near active zones in snake motor boutons. J Neurosci 20:7986–7993.

Wu Y, He Y, Bai J, Ji SR, Tucker WC, Chapman ER, Sui SF (2003) Visualization of synaptotagmin 1 oligomers assembled onto lipid monolayers. Proc Natl Acad Sci U S A 100:2082–2087.

Yamashita T, Hige T, Takahashi T (2005) Vesicle endocytosis requires dynamin-dependent GTP hydrolysis at a fast CNS synapse. Science 307:124–127.

Zhang JZ, Davletov BA, Südhof TC, Anderson RG (1994) Synaptotagmin 1 is a high affinity receptor for clathrin AP-2: implications for membrane recycling. Cell 78:751–760.